Observational Study

Medicine®

OPEN

The 360° circumferential opening of Schlemm's canal in normal individuals detected by enhanced depth imaging optical coherence tomography

Sili Jing, MD, Zhiqi Chen, PhD, Wei Chen, PhD, Hong Zhang, PhD, Junming Wang, PhD*

Abstract

We aimed to observe the opening status and morphological parameters of Schlemm's canal (SC) in normal eyes using enhanced depth imaging optical coherence tomography (EDI-OCT).

Consecutive EDI-OCT scans were used to examine the right eye of 20 normal individuals. EDI-OCT was performed clockwise for 8 regions (at the 12:00, 1:30, 3:00, 4:30, 6:00, 7:30, 9:00 and 10:30 o'clock positions). Image processing and analysis in java software was used to measure the area, perimeter, and diameter of SC. Twenty-one serial scans of each region were evaluated and a total of 168 images were included in the analyses of each eye.

The SC was detected in 100.0% of the sections. The distribution of individual measurements of SC was highly variable. The mean values of SC size significantly differed among the different clock-face positions. The mean values of the area, perimeter, and diameter of SC in the 9:00 o'clock position were the lowest, and those at the 7:30 o'clock position were the highest ($P < .05$). There was no obvious association between intraocular pressure and SC size at any clock position.

Although SC tends to open circumferentially in normal individuals, the distribution of individual measurements is highly variable. Morphological manifestation of SC measured by EDI-OCT is a useful way to evaluate the circumferential opening status of SC.

Abbreviations: BCVA = the best corrected visual acuity, EDI-OCT = enhanced depth imaging optical coherence tomography, IOP = intraocular pressure, OCT = optical coherence tomography, SC = Schlemm's canal, TM = trabecular meshwork, UBM = ultrasound biomicroscopy.

Keywords: circumferential opening, normal individuals, optical coherence tomography, Schlemm's canal

1. Introduction

In the normal eye, the drainage pathway of the aqueous humor contains the trabecular meshwork (TM), Schlemm's canal (SC), collector channels, and episcleral veins.[1–3] As the central resistance point of the aqueous pathway in the eye, the SC, collector channels, and the episcleral venous system account for approximately 50% of decrease in the aqueous outflow.[4] At the level of SC, several changes in glaucomatous eyes have been observed with the potential to be a significant contributor to the increased outflow resistance.[5–8] It is therefore very important to investigate the microstructure of SC to clarify its effect on the outflow resistance.

Optical coherence tomography (OCT) is a non-invasive technique that can detect microstructural changes in the anterior chamber angle in vivo, including the size of the SC.[9,10] Many previous studies have used OCT to measure the superior, inferior, nasal, and temporal SC size.[11,12] However, only four points in the SC circle have been examined, and the exact opening status of SC circumferentially in normal individuals remains uncertain.

Enhanced depth imaging OCT (EDI-OCT) is an advanced technique to observe SC, and the scan direction of the anterior segment module can be adjusted circumferentially to make OCT scans perfectly perpendicular to the limbus.[13] Therefore, in this study, to describe the circumferential opening status and morphological parameters of SC in normal individuals, we used EDI-OCT to scan SC at 8 positions circumferentially, and analyzed 21 serial scans of each position.

2. Materials and methods

This observational study was approved by the Ethics Committee of the Tongji Hospital, Tongji Medical College, Huazhong University of Science and Technology, Wuhan, China and adhered to the tenets of the declaration of Helsinki. Written informed consent was obtained from all the participants prior to enrollment in the study.

Editor: Xiong Kun.

SJ and ZC contributed equally to the work presented here and should therefore be regarded as equivalent authors.

This study was supported by the National Natural Science Foundation of China (Grant 81974133 and 81470632).

The authors have no conflicts of interest to disclose.

Department of Ophthalmology, Tongji Hospital, Tongji Medical College, Huazhong University of Science and Technology, Wuhan, China.

** Correspondence: Junming Wang, Department of Ophthalmology, Tongji Hospital, Tongji Medical College, Huazhong University of Science and Technology, Wuhan 430030, China (e-mail: eyedrwjm@163.com).*

How to cite this article: Jing S, Chen Z, Chen W, Zhang H, Wang J. The 360° circumferential opening of Schlemm's canal in normal individuals detected by enhanced depth imaging optical coherence tomography. Medicine 2020;99:7 (e19187).

Received: 12 September 2019 / Received in final form: 27 December 2019 / Accepted: 14 January 2020

http://dx.doi.org/10.1097/MD.0000000000019187

2.1. Subjects and imaging processing

Twenty employees of Tongji Hospital were enrolled in this study. All participants underwent an ophthalmic examination, including measurement of The best corrected visual acuity (BCVA), refractive error, intraocular pressure (IOP; NIDEK non-contact tonometer RT-2100, www.nidek.com), and central corneal thickness, slit-lamp examination, and fundus examination. The inclusion criteria for these healthy volunteers were as follows: age 20 to 40 years, BCVA ≥ 20/25 (0.10 logMAR, metric Snellen 6/7.5), refractive error between +3.0 and −6.0 D, IOP between 10 and 21 mmHg, and normal optic disc and retina (Table 1). The exclusion criteria were as follows: history of IOP > 21 mm Hg, vitreoretinal disease, uveitis, and history of intraocular surgery or systemic diseases such as hypertension and diabetes that would potentially affect the eyes.

EDI-OCT (Spectralis, Heidelberg Engineering GmbH, Dossenheim, Germany) was used to examine the right eye of each subject. Scans were performed clockwise for the eight regions (at the 12:00, 1:30, 3:00, 4:30, 6:00, 7:30, 9:00 and 10:30 o'clock positions). For a rectangular area of 15 × 5°, 21 serial EDI-OCT B-scans were obtained (20 frames were stacked to generate one EDI-OCT B-scan). All OCT scans were performed under standardized darkroom photopic conditions (ca. 3.5 lux) by the same examiner (Wei Chen).

2.2. Measurement of SC

SC was regarded as a round tubular structure with low-density shadow on the triangular TM (Fig. 1). As reported in our previous study,[12,14,15] image processing and analysis in Java (ImageJ) software (version 1.45S, National Institutes of Health, Available at: http://imagej.nih.gov/ij/) was used to measure the area, perimeter, and diameter of SC. Twenty-one serial scans of each region were measured. The measurement was repeated three times and the average values were recorded and stored for statistical analysis. To measure the intraobserver repeatability and interobserver reproducibility (Sili Jing and Zhiqi Chen), 30 images were randomly chosen from 5 subjects for the analysis using a two-way mixed effect model.

2.3. Statistical analyses

All statistical analyses were performed using the SPSS software (version 16.0; SPSS, Inc., Chicago, IL). The data were presented as the mean ± standard deviation. The Student *t* test was used for comparisons of different SC parameters between different regions. Nonparametric Pearson correlation analyses were performed to examine the relationships between IOP and SC parameters. Statistical significance was defined as $P < .05$ and all tests were 2-tailed.

Table 1

Baseline characteristics of all the subjects.

Age, yr	
Mean (SD)	28.4 (3.9)
Gender (Male:Female)	10:10
RE(D)	
Mean (SD)	-2.75D (-1.75)
Max	-5.75D
Min	-0.25D
IOP(mm Hg)	
Mean (SD)	14.8 (2.4)
Max	19.3
Min	11.7

Data are presented as mean ± SD.
IOP = intraocular pressure, RE = refractive error, SD = standard deviation.

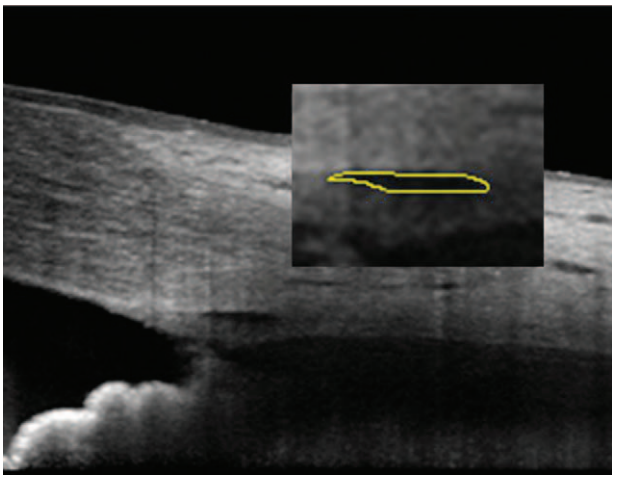

Figure 1. The yellow curve indicates the area of SC. SC = Schlemm's canal.

3. Results

The study included 20 subjects (10 male; 10 female. Table 1). For each eye, 8 quadrants were measured, with 21 scans per quadrant, totaling to 3360 images in the analysis. The mean age was 28.4 years (range, 22–38 years). The mean IOP was 14.75 mm Hg (range, 11.7–19.3 mm Hg), and the mean refractive error (RE) was -2.75 D (range, -0.25 – -5.75 D). All OCT measurements showed excellent reproducibility and repeatability (all $P < .05$).

The SC was observable in 100.0% of sections (Fig. 2). The distribution of individual measurements of SC was highly variable (Tables 2–4). The mean values of the size of SC differed significantly for some positions. The mean area of SC in the 9:00 o'clock position (5582.4 ± 1638.6 um^2) was the lowest and that at the 7:30 o'clock position (7351.5 ± 1701.1 um^2) was the highest (Fig. 3). The mean perimeter of SC in the 9:00 o'clock position (525.9 ± 132.9 um) was the lowest and that in the 7:30 o'clock position (616.3 ± 97.7 um) was the highest (Fig. 4). The mean diameter of SC in the 9:00 o'clock position (251.8 ± 72.8 um) was the lowest, and that at the 7:30 o'clock position (297.9 ± 56.2 um) was the highest (Fig. 5).

There was no obvious association between IOP and SC size at different positions.

4. Discussion

In this study, we showed that the SC tended to open in 8 positions. The mean value of SC size in the 9:00 o'clock position was the smallest, and that at the 7:30 o'clock position was the largest. Our results provide detailed physiological data for circumferential SC size.

In previous studies, ultrasound biomicroscopy (UBM) had been used to investigate SC size in the superior, inferior, nasal, and temporal regions.[16–19] UBM could provide a continuous and intuitive imaging of SC, but the contact examination of UBM may cause eye discomfort and even corneal injury. In addition,

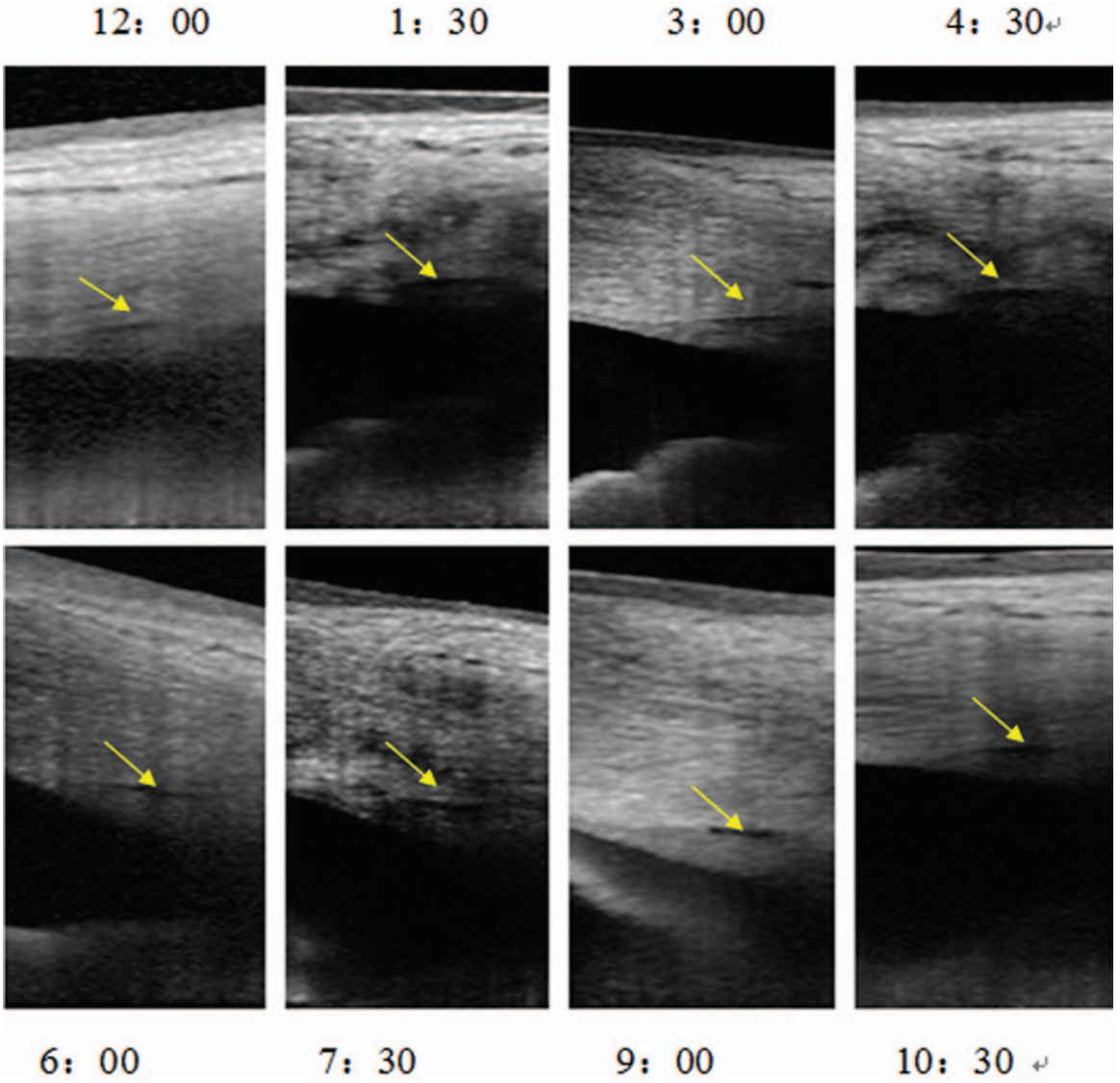

Figure 2. The SC was observable in each quadrant. SC = Schlemm's canal.

the external force on the eyeball during UBM examination may influence the SC size on the scans. Therefore, non-invasive EDI-OCT used in our study is a safer and more accurate technique to be used in the clinical setting.

The rate of observation of SC in normal individuals has been evaluated in different studies.[12,16,20] In our previous report, in children aged 7 to 14 years, SC was observable in 100% of the sections, whereas it was observable in 80.6% of the sections in those aged 60 to 83 years.[12] Yan X et al used 80-MHz UBM to measure the SC in the superior, inferior, nasal, and temporal regions, and reported the observation rate as 80.3% in normal individuals.[16] Kai Gao et al used the same OCT device to show that the rate of detection of SC was highest in the superior quadrant (85.3%) and lowest in the inferior quadrant (75.5%).[20] However, in our study, SC was detected in all the scans at every scan position. We speculated that in previous UBM and OCT studies, only one image of each position was used for analysis, which may have resulted in obscure outlines of SC. In this study, however, we used 21 sequential OCT B-scans in each position to judge the SC outline. Interestingly, we noted that SC in normal individuals had a 360° circumferential opening.

Many studies have reported that the TM and SC pathway are responsible for segmental outflow.[21–23] Elliott D.K. Cha et al used confocal microscopy and global imaging to analyze areas of active outflow based on the distribution of a fluorescent tracer in the TM and SC, and proved that the SC conserved a segmental outflow.[21] We therefore hypothesized that the SC opens circumferentially and has a dominant as well as non-dominant drainage area. Aqueous humor preferentially flows out from the dominant drainage area of the SC with less friction, which may be related to the heavy distribution of collector channels within the dominant drainage area; as a result, fluorescent tracers can be more easily found in the dominant drainage area.[24,25] On the contrary, less aqueous humor flows out from the non-dominant drainage area of the SC because of greater friction. Fluorescent tracers are therefore lesser in the non-dominant drainage area despite the SC being open. Therefore, it would be very meaningful to further study the association between SC morphology and function.

Table 2

The SC area existed no obvious regularity at 8 positions of all subjects. 1 to 20 represented serial number of all the subjects. SC = Schlemm's canal.

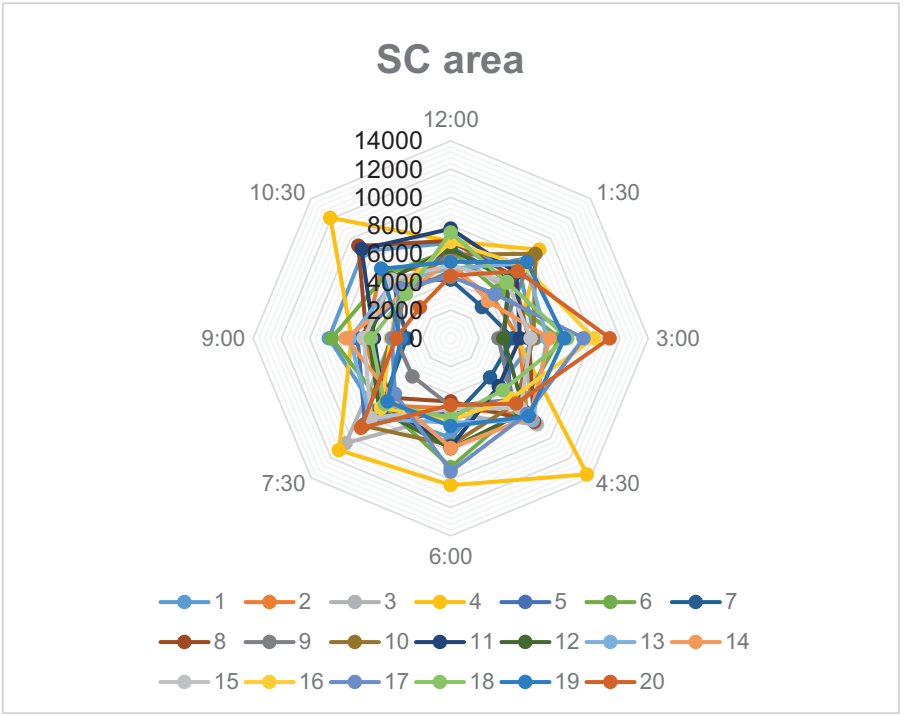

Table 3

The SC perimeter existed no obvious regularity at 8 positions of all subjects. 1 to 20 represented serial number of all the subjects. SC = Schlemm's canal.

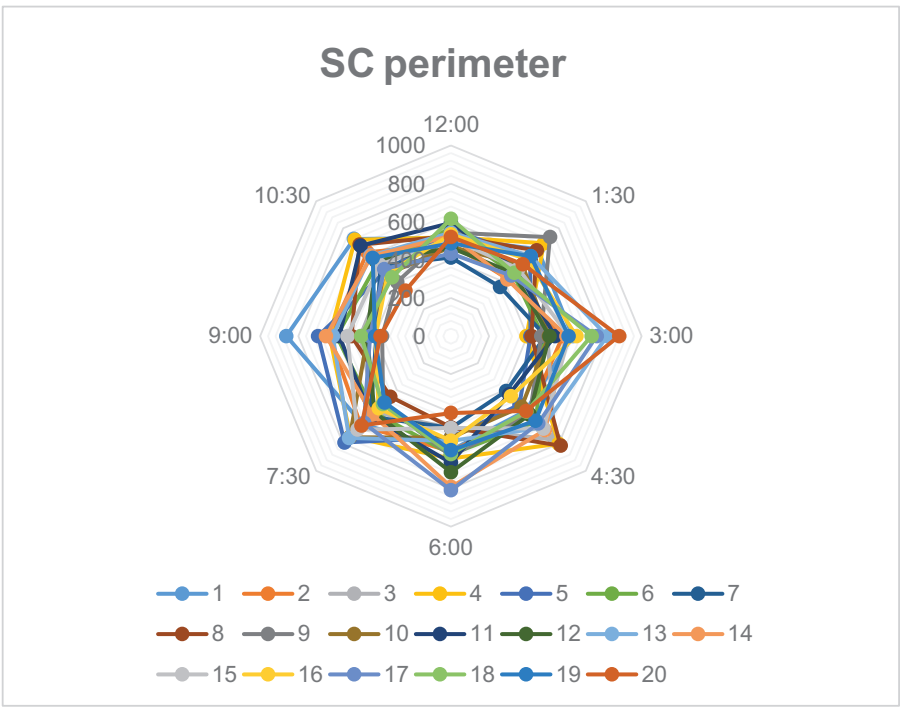

Table 4

The SC diameter existed no obvious regularity at 8 positions of all subjects.1 to 20 represented serial number of all the subjects. SC = Schlemm's canal.

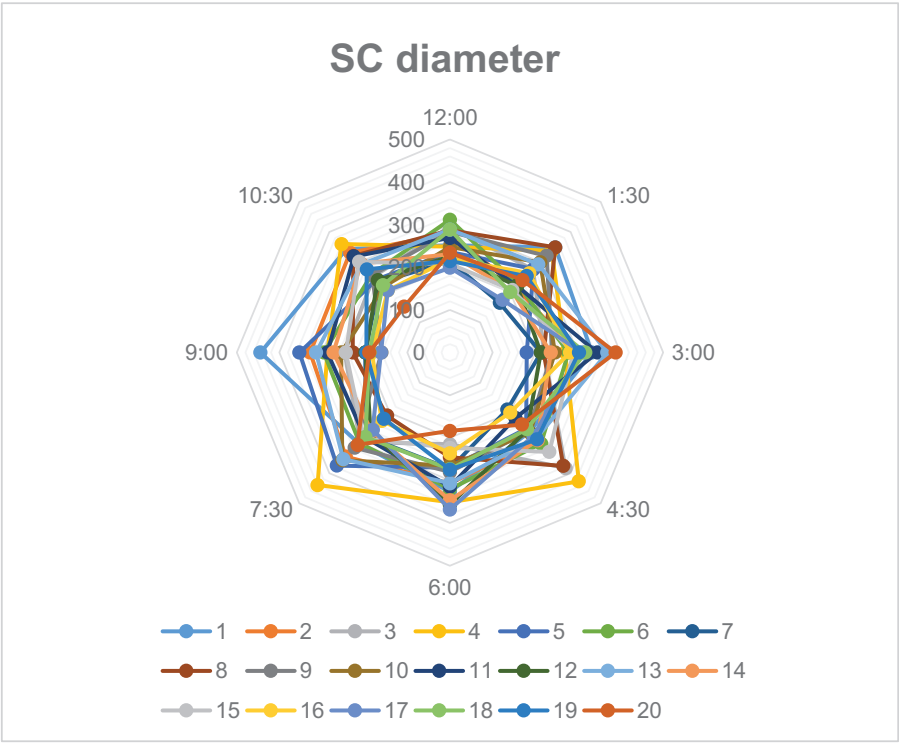

In our study, the mean area of SC in the 9:00 o'clock position was the smallest and that in the 7:30 o'clock position was the largest, which was inconsistent with the results of other studies.[8,11] Larry Kagemann et al reported that SC area in the nasal position was significantly larger than that at the temporal position.[8] Guohua Shi et al reported that the area, diameter, and perimeter of SC exhibited no significant differences between the nasal and temporal positions.[11] This discrepancy may have resulted from the number of scans analyzed in the studies (21 serial scans of each region in our study versus only one scan in other studies).

The distribution of individual measurements of SC was highly variable in our study and we speculated that different groups of individuals or different sample sizes may have led to these results. Thus, the tendency of variation of SC in different positions is uncertain and further investigations are needed to confirm our study findings.

This study has some limitations. First, all subjects in our study were young adults and it is unclear if the characteristics of SC would be similar in elderly subjects. Second, because of the limitation of large data processing, we only measured 8 positions in each eye; however, in the

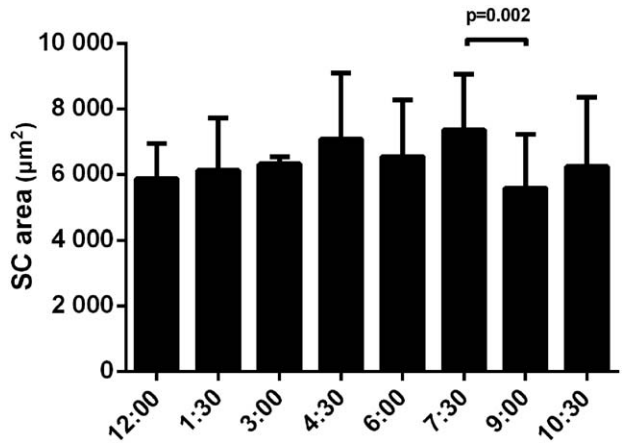

Figure 3. The statistical difference of the mean values of SC area among different positions. SC = Schlemm's canal.

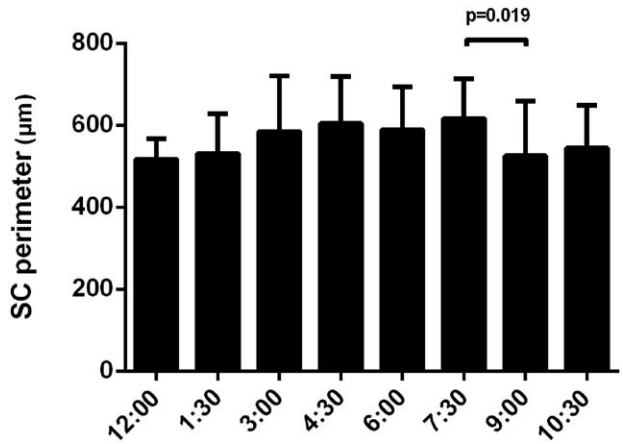

Figure 4. The statistical difference of the mean values of SC perimeter among different positions. SC = Schlemm's canal.

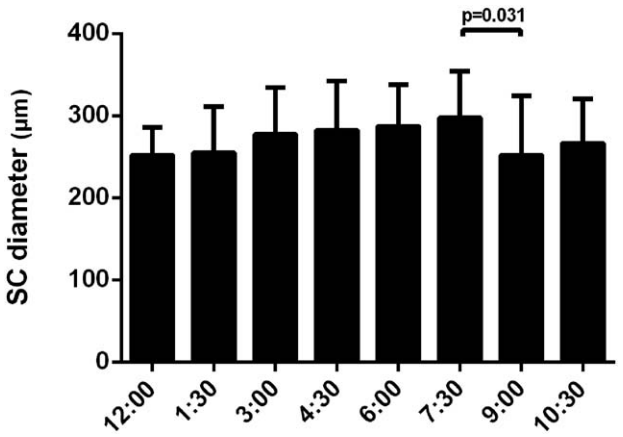

Figure 5. The statistical difference of the mean values of SC diameter among different positions. SC = Schlemm's canal.

future, we aim to measure all the positions of SC circumferentially.

5. Conclusions

Using EDI-OCT, we revealed that SC tends to open circumferentially in normal individuals. EDI-OCT is a useful method to investigate the morphology of SC. It could help evaluate the differences between normal eyes and those with glaucoma, in turn providing helpful information for glaucoma surgery.

Author contributions

Sili Jing, Zhiqi Chen and Wei Chen performed the research and data analysis. Sili Jing and Zhiqi Chen wrote the main manuscript text. Hong Zhang and Junming Wang designed the study and revised the manuscript. All authors reviewed the manuscript.

References

[1] Hann CR, Vercnocke AJ, Bentley MD, et al. Anatomic changes in Schlemm's canal and collector channels in normal and primary open-angle glaucoma eyes using low and high perfusion pressures. Invest Ophthalmol Vis Sci 2014;55:5834–41.
[2] Tamm ER. The trabecular meshwork outflow pathways: structural and functional aspects. Exp Eye Res 2009;88:648–55.
[3] Francis AW, Kagemann L, Wollstein G, et al. Morphometric analysis of aqueous humor outflow structures with spectraldomain optical coherence tomography. Invest Ophthalmol Vis Sci 2012;53:5198–207.
[4] Rosenquist R, Epstein D, Melamed S, et al. Outflow resistance of enucleated human eyes at two different perfusion pressures and different extents of trabeculotomy. Curr Eye Res 1989;8:1233–40.
[5] Allingham RR, de Kater AW, Ethier CR. Schlemm's canal and primary open angle glaucoma: correlation between Schlemm's canal dimensions and outflow facility. Exp Eye Res 1996;62:101–9.
[6] Forgáčová V, Lešťák J, Pitrová S, et al. Schlemm's canal in OCT images in glaucoma patients and healthy subjects. J Clin Exp Ophthalmol 2013;4:292.
[7] Alvarado JA, Murphy CG. Outflow obstruction in pigmentary and primary open angle glaucoma. Arch Ophthalmol 1992;110:1769–78.
[8] Kagemann L, Wollstein G, Ishikawa H, et al. Identification and assessment of Schlemm's canal by spectral-domain optical coherence tomography. Invest Ophthalmol Vis Sci 2010;51:4054–9.
[9] Hong J, Xu J, Wei A, et al. Spectral-domain optical coherence tomographic assessment of Schlemm's canal in Chinese subjects with primary open-angle glaucoma. Ophthalmology 2013;120:709–15.
[10] Imamoglu S, Sevim MS, Alpogan O, et al. In vivo biometric evaluation of Schlemm's canal with spectral-domain optical coherence tomography in pseudoexfoliation glaucoma. Acta Ophthalmol 2016;94:e688–92.
[11] Shi G, Wang F, Li X, et al. Morphometric measurement of Schlemm's canal in normal human eye using anterior segment swept source optical coherence tomography. J Biomed Opt 2012;17:016016.
[12] Chen Z, Sun J, Li M, et al. Effect of age on the morphologies of the human Schlemm's canal and trabecular meshwork measured with swept source optical coherence tomography. Eye (Lond) 2018;32:1621–8.
[13] Spaide RF, Koizumi H, Pozzoni MC. Enhanced depth imaging spectral-domain optical coherence tomography. Am J Ophthalmol 2008;146:496–500.
[14] Chen W, Chen L, Chen Z, et al. Influence of the water-drinking test on intraocular pressure, Schlemm's canal, and autonomic nervous system activity. Invest Ophthalmol Vis Sci 2018;59:3232–8.
[15] Chen Z, Song Y, Li M, et al. Schlemm's canal and trabecular meshwork morphology in high myopia. Ophthalmic Physiol Opt 2018;38:266–72.
[16] Yan X, Li M, Chen Z, et al. Schlemm's canal and trabecular meshwork in eyes with primary open angle glaucoma: a comparative study using high-frequency ultrasound biomicroscopy. PLoS One 2016;11:e0145824.
[17] Yan X, Li M, Song Y, et al. Influence of exercise on intraocular pressure, Schlemm's canal, and the trabecular meshwork. Invest Ophthalmol Vis Sci 2016;57:4733–9.
[18] Irshad FA, Mayfield MS, Zurakowski D. Variation in Schlemm's canal diameter and location by ultrasound biomicroscopy. Ophthalmology 2010;117:916–20.
[19] Dada T, Gadia R, Sharma A, et al. Ultrasound biomicroscopy in glaucoma. Surv Ophthalmol 2011;56:433–50.
[20] Gao K, Li F, Aung T. Diurnal variations in the morphology of Schlemm's canal and intraocular pressure in healthy Chinese: an SS-OCT study. Invest Ophthalmol Vis Sci 2017;58:5777–82.
[21] Cha ED, Xu J, Gong L. Variations in active outflow along the trabecular outflow pathway. Exp Eye Res 2016;146:354–60.
[22] Carreon TA, Edwards G, Wang H, et al. Segmental outflow of aqueous humor in mouse and human. Exp Eye Res 2017;158:59–66.
[23] Vranka JA, Bradley JM, Yang Y-F, et al. Mapping molecular differences and extracellular matrix gene expression in segmental outflow pathways of the human ocular trabecular meshwork. PLoS ONE 2015;10:e0122483.
[24] Battista SA, Lu Z, Hofmann S, et al. Reduction of the available area for aqueous humor outflow and increase in meshwork herniations into collector channels following acute IOP elevation in bovine eyes. Invest Ophthalmol Vis Sci 2008;49:5346–52.
[25] Lu Z, Zhang Y, Freddo TF, et al. Similar hydrodynamic and morphological changes in the aqueous humor outflow pathway after washout and Y27632 treatment in monkey eyes. Exp Eye Res 2011;93:397–404.